Proceedings of the
Annual Stability Conference
Structural Stability Research Council
Orlando, Florida, April 12-15, 2016

Improved Stability Design of Longitudinally Stiffened Plate Girders

Lakshmi Subramanian[1], Donald W. White[2]

Abstract

Longitudinal stiffeners are welded to the webs of slender-web I-girders to restrict the web lateral deformations at service and construction load levels. The AASHTO 2015 equations recognize an increase in the bend-buckling resistance of girder webs reinforced by longitudinal stiffeners. However, in girders where web bend-buckling occurs prior to reaching the girder ultimate flexural resistance, a portion of the web becomes ineffective and flexural stresses are re-distributed largely to the compression flange. The current Specification equations impose a penalty on the strength of the compression flange by a load shedding factor, R_b. However, this load shedding factor neglects the contribution of the longitudinal stiffener to the web post-buckling resistance. The authors have previously developed a cross-section model that can be used to estimate the flexural capacity of I-girders for both homogenous and hybrid girders at the yield limit state. In this paper, an improved handling of combined web buckling and lateral torsional buckling of longitudinally stiffened plate girders is proposed based on finite element test simulations. In addition, the R_b calculated from the proposed model, used in conjunction with the current Specification flange local buckling equations is shown to provide a better characterization of the flange local buckling capacity of longitudinally stiffened I-girders.

1. Introduction

Plate girders used in longer-span bridges typically have slender webs combined with longitudinal stiffening to prevent theoretical web bend-buckling during construction and under service loads. The current American Association of State Highway and Transportation Officials Load and Resistance Factor Design Specifications (AASHTO LRFD) (AASHTO 2015) require the use of longitudinal stiffeners on plate girders when the web slenderness D/t_w *is* greater than 150. In addition to the above considerations, this requirement is largely to alleviate web distortion induced fatigue concerns. The bend-buckling resistance of a longitudinally stiffened plate girder web is higher than that of an unstiffened web. However, for cases where the longitudinally-stiffened web bend-buckling resistance (i.e., the web local buckling resistance under flexural compression) is exceeded by the strength loading combinations, AASHTO LRFD currently

[1] Post-Doctoral Research Affiliate, Georgia Institute of Technology, <pslakshmipriya@gatech.edu>
[2] Professor, Georgia Institute of Technology, <dwhite@ce.gatech.edu>

neglects the beneficial influence of the longitudinal stiffeners in determining the contribution of the postbuckled web to the girder flexural resistance. This is due to the fact that the AASHTO provisions for proportioning of the longitudinal stiffeners do not consider the strength behavior of stiffened web panels in the postbuckled condition. The longitudinal stiffener design rules consider only the restraining effects of the longitudinal stiffeners on the theoretical bend-buckling resistance of the web panels.

Once a girder's web bend buckles, the portion of the web in compression becomes less effective in carrying additional load and the corresponding flexural stresses are shed largely to the girder's compression flange. The stress variation through the depth of the web becomes highly nonlinear at postbuckling load levels. The term R_b in AASHTO (2015) is a reduction factor on the flexural resistance of the compressive flange that accounts for this load shedding from the web. The tension flange stresses are not significantly impacted by load shedding from the web (Basler and Thurliman 1961), and the AASHTO provisions do not consider any strength reduction in the flexural checks of the tension flange. The current AASHTO LRFD Specification requirements for R_b neglect the contribution of the longitudinal stiffeners toward the development of the girder post-web buckling flexural resistance. This can have a significant impact in regions of negative flexure. R_b is given by AASHTO equation 6.10.1.10.2-3,

$$R_b = 1 - \left(\frac{a_{wc}}{1200 + 300 a_{wc}} \right) \left(\frac{2D_c}{t_w} - \lambda_{rw} \right) \leq 1.0 \tag{1}$$

which was suggested originally by Basler and Thurliman for non-longitudinally stiffened doubly-symmetric girders, but used in the same form for singly-symmetric girders as well. In the equation, a_{wc} is the ratio of two times the web area in compression to the area of the compression flange, D_c is the web depth in compression, t_w is the thickness of the web, and λ_{rw} is the noncompact web slenderness limit.

The authors have conducted extensive parametric studies using finite element (FE) test simulations in ABAQUS (Simulia 2013) on longitudinally stiffened girders with different cross-sectional properties (principally, web depth-to-thickness ratio, web depth-to-compression flange width ratio, web depth in compression, transverse stiffener spacing, thickness of flange-to-thickness of web ratio, longitudinal stiffener lateral rigidity, longitudinal stiffener width-to-thickness ratio, position of the longitudinal stiffener relative to the web depth, and area of longitudinal stiffener-to-area of web) and proposed a cross-section model (R_b model) that can be used to estimate the ultimate flexural capacity of longitudinally stiffened girders (Subramanian and White 2016). The cross-section model, which is reviewed in the following section is derived based on longitudinally stiffened members subjected to uniform moment and failing at the yield limit state, i.e. lateral torsional buckling (LTB) and flange local buckling (FLB) are prevented by the selection of the flange width-to-thickness ratio and sufficient spacing of lateral braces.

This paper assesses the applicability of the proposed R_b model to the LTB and FLB flexural limit states. This is done via uniform moment studies on homogenous girders. An improved handling of combined web flexural buckling and LTB is proposed here, with the aid of the proposed R_b model. In addition, this paper also shows that using the R_b computed from the proposed model in conjunction with the AASHTO 2015 Specification equations provides a much improved estimation of FLB resistance of longitudinally stiffened girders.

2. R_b for Longitudinally Stiffened Girders

This section summarizes the results from extensive studies on longitudinal stiffened girders of different cross-section parameters (Subramanian and White 2016). The model shown in Fig. 1 is proposed for calculating the flexural capacity of longitudinally stiffened members at the yield limit state. The model is applicable for both homogenous girders (equal yield strength web, flange and longitudinal stiffener plates), and hybrid girders (higher yield strength flange plates, equal yield strength web and longitudinal stiffener plates). Figure 1 indicates the portion of the web in the two sub-panels that is effective at the yield limit state. Figure 2 shows the variation of normal stresses through the depth of the web (averaged through the web thickness) for different depths of the web in compression for girders with web depth-to-thickness ratio, D/t_w = 240 and d_o/D = 1, where d_o is the transverse stiffener spacing. This is representative of the general trend in all the girders that were studied. It may be surmised from this figure that the nominal elastic depth of the web in compression, D_c* (calculated based on the equilibrium and strain compatibility, using the compressive stress distribution shown), is a reasonable estimate of the location of the neutral axis in the physical girder.

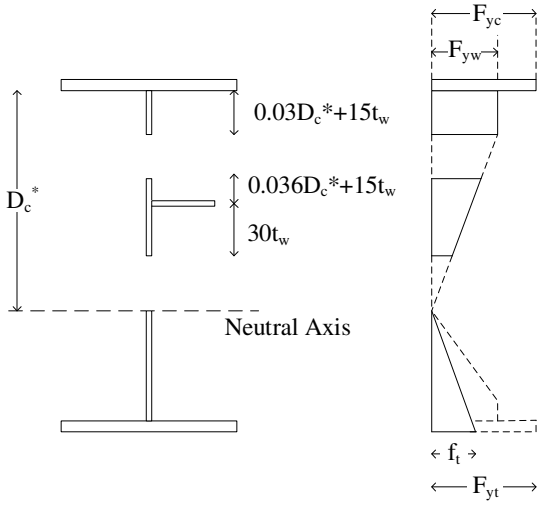

Figure 1: Cross-section model to calculate R_b of longitudinally stiffened girder

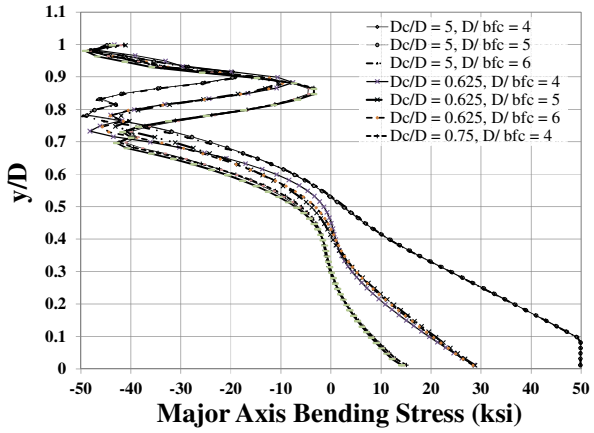

Figure 2: Major axis bending stresses in the web, averaged through the web thickness, for homogenous girders with D/t_w = 240; y is the distance from the bottom of the web, D is the total web depth

Figure1 provides an approximation of the stress distributions obtained in Fig.2, and can be used to determine the yield limit state flexural resistance of the girder using basic strength of materials concepts. The compressive stresses to be used in the flexural capacity calculations are as shown in Fig.1. The depth of the web in compression, D_c*, is calculated via an iterative process that satisfies equilibrium and strain compatibility. It is found that the moment of the area of the longitudinal stiffener about the calculated neutral axis should be included in the calculation of the cross-sectional flexural resistance. One can determine the internal moment produced by the assumed stress distribution based on either one of the following assumptions that satisfies equilibrium (sum of longitudinal forces equal to zero):

1. The entire section is elastic on the tension side of the neutral axis. In this case, the elastic stress distribution below the neutral axis is scaled such that the total longitudinal force in the cross-section is equal to zero.
2. Nominal yielding is reached at some depth on the tension side of the neutral axis. In this case, the section is assumed to have a constant tensile stress equal to F_{yw} below this depth in the web, and F_{yt} or f_t in the tension flange (depending on whether or not the tension flange is yielded), and a linearly varying elastic stress distribution above this depth up to the neutral axis.

The web bend-buckling factor from the proposed model, R_{bPr} is determined as the ratio of the flexural resistance of the effective cross-section shown in Fig.1 to the yield moment capacity of the gross cross-section, including the contribution of the longitudinal stiffener (M_{nPr}/M_y).

It is further recommended that the contribution of the longitudinal stiffener to the postbuckling flexural resistance of the girder be neglected within the panel(s) containing the discontinuity when the longitudinal stiffeners are discontinuous across transverse stiffeners.

The following sections detail how the above R_b model may be applied to the LTB and FLB limit states.

3. FE Modeling Parameters

3.1 FE Discretization

In this research, full nonlinear analyses are conducted to simulate physical tests using ABAQUS(Simulia 2013). The flanges, web and longitudinal stiffener are modeled using four-node shell elements degenerated from a 3D solid element (the S4R shell element). Intermediate transverse stiffeners are modeled using compatible B31 beam elements. The mesh is dense with 60 elements through the web depth, and 12 elements across the width of the flanges, and 10 elements along the width of the longitudinal stiffener. The aspect ratio of the shell elements in the web is approximately equal to 1.0.

3.2 Material Modeling

In this paper, all members are considered to be homogenous and the yield stress of the steel, F_y, is taken as 50 ksi. The modulus of elasticity, E is taken as 29000 ksi. The material is modeled with a small tangent stiffness within the yield plateau region of E/1000 up to a strain-hardening strain of $\varepsilon_{sh} = 10\varepsilon_y$, where ε_y is the yield strain of the material. Beyond this strain, a constant strain-hardening modulus of $E_{sh} = E/50$ is used. The maximum longitudinal strains reached in these studies is seldom in the order of 2 to 3 ε_y.

3.3 Test Setup

The straight girders in this study are subjected to four-point bending with the test specimen subjected to uniform bending and flanked by an end fixture on each side. The test setup is similar to that used in Cooper's experiments (Cooper 1965) and is shown in Fig. 3. The unbraced lengths of the test specimens are varied to allow evaluation of the impact of the longitudinal stiffener on the flexural capacity of girders subjected to the yield, inelastic LTB, and elastic LTB limit states. The test fixtures are assumed to provide torsionally and laterally fixed boundary conditions at each end of the specimen, i.e., the value of K in KL_b is taken as 0.5 in estimating the LTB resistances by various potential nominal strength equations. The flange and web plates of the end fixtures are significantly larger than the plate thicknesses of the test specimens; therefore, this is an accurate estimate of K. The length L_b is taken as the distance between the connection points to the end fixtures (i.e., no lateral bracing is provided within the length of the test specimens, but lateral bracing is provided at the ends of the test specimens).

In the FLB tests, lateral bracing is located within the test specimen such that the unbraced lengths are smaller than the plateau length, L_p.

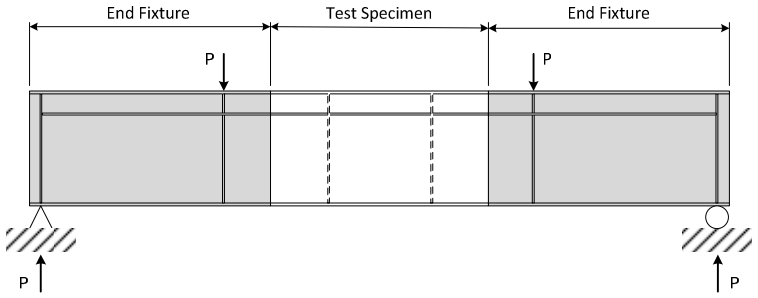

Figure 3: Test setup

3.4 Initial Geometric Imperfections

Figure 4 shows the initial web out-of-flatness, flange sweep and flange tilt imperfections assumed in this work. The flange tilt is not considered in the LTB studies (only compact flange cross-sections are considered), and the flange sweep is not considered in the FLB studies (since closely-spaced bracing was employed in the FLB studies). AWS (2010) allows a maximum web out-of-flatness of 1/67 times the least panel dimension for girders with longitudinal stiffeners and a flange tilt equal to the smaller of $b_{fc}/100$ and 2.5 in. In addition, AWS effectively allows a maximum flange out-of-straightness of $L_b/960$, where L_b is the unbraced length of the member. The maximum out-of-straightness permitted in the AISC COSP(AISC 2010) is effectively $L_b/1000$. Given the fixity at both ends of the unbraced length, a flange sweep imperfection of magnitude $L_b/1000$ amounts to a smaller net imperfection between the inflection points of the unbraced length, and is nearly equal to half the AWS tolerance. It is shown by Subramanian and White (2015; 2015a) that the use of the full tolerance values in FE simulations may be overly conservative relative to the experimental data represented by the AISC/AASHTO LTB curves, and that one-half the AWS tolerances yields better correlation with experimental data comprising of unstiffened girders. A comparison is shown in the following section, using one-half and the full tolerances (for the case of one-half tolerances, the maximum imperfection magnitudes are taken as one-half of that shown in Fig. 4 (a), (b), and (c)). The sweep in the longitudinal stiffener is taken as $d_o/400$ (Hendy and Murphy 2007) without reducing to one-half its magnitude.

The test simulations are first run using the base imperfection pattern shown in Fig. 4(a) along with either the flange tilt or sweep as appropriate for the expected failure mode, and the limit load and failure mode is determined from these analyses. The web lateral deflection at the limit load, which is taken as the failure mode pattern, is then scaled as described below to form the actual imperfection for the final test simulation analysis. In other words, the test simulation is run twice; once with the base imperfection pattern shown in Fig. 4(a) as the initial geometric imperfection, and then a second time by using the failure mode from the first analysis, scaled to satisfy the AWS (2010) tolerances on the maximum web out-of-flatness, as the initial imperfection. The flange sweep or flange tilt are also scaled as per the AWS tolerances. This relatively elaborate procedure is similar to an approach recommended by Hendy and Murphy (2007), and is believed to provide a reasonable estimate of the worst-case geometric imperfections for calculation of the "true R_b" of the test girders. The base web out-of-flatness shown in Fig. 4(a) is used as the starting point for the above analyses after conducting imperfection sensitivity studies (Subramanian and White 2014) with various base imperfection patterns and magnitudes.

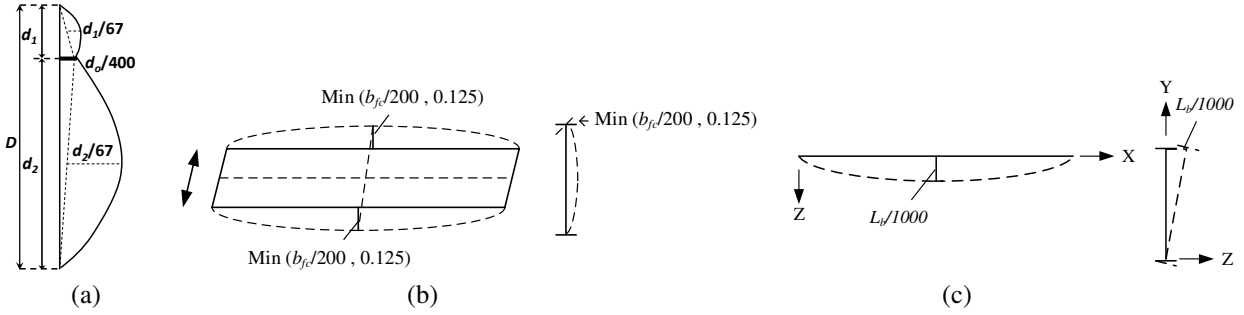

Figure 4: Initial geometric imperfections (a): Base imperfection for web out-of-flatness and longitudinal stiffener sweep (b): Flange tilt imperfection (c): Flange sweep

3.5 Residual Stresses

The residual stresses used in the studies are shown in Fig. 5. Residual stresses in the slender webs are neglected as they are small enough to cause negligible effect on the flexural capacities of slender web longitudinally stiffened plate girders (Subramanian and White 2014). The flange residual stress distribution is based on the Best-Fit Prawel pattern (Kim 2010).

A self-equilibrating residual stress pattern in the longitudinal stiffener is developed based on an assumed heat affected zone of $b_l/5$, where, b_l is the width of the longitudinal stiffener. This pattern is obtained by starting with a typical residual stress pattern where the heat-affected zone has a tensile residual stress equal to F_y and the rest of the plate has a self-equilibrating residual compression. The elastic flexural stresses necessary to put this plate in moment equilibrium are then added to the above base stresses to create a representative statically admissible residual stress distribution in the longitudinal stiffener.

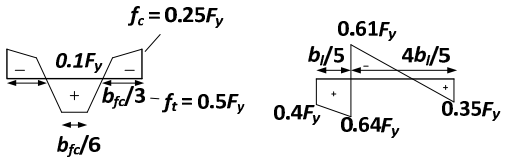

(a) Flanges (b) Longitudinal stiffener

Figure 5: Residual stress patterns

4. Lateral Torsional Buckling Limit State

4.1 Proposed LTB Model for Longitudinally Stiffened Girders

A modified form of the AASHTO (2015) Specification equations for LTB is proposed by Subramanian and White (2016; 2015b; 2015c) after extensive studies encompassing FE simulations of unstiffened rolled and welded members (both homogenous and hybrid) subjected to uniform moment and moment gradient loading, along with statistical and reliability analysis of a large experimental database. As per the recommendations, the LTB strength curve uses a plateau length of $L_p = 0.63 r_t \sqrt{E / F_y}$ (where L_p is the largest unbraced length at which the cross-section attains its full capacity without undergoing significant lateral torsional buckling, r_t is the effective radius of gyration for LTB), and a smaller maximum stress level for elastic LTB of F_{yr} = 0.5 F_{yc}. This model, with the modifications discussed below to address the influence of web longitudinal stiffening, is proposed in this paper as one method that captures the test simulation results for longitudinally stiffened girders with improved accuracy. Furthermore, for the longitudinally stiffened plate girders considered in this research, the "plateau" resistance used with these equations is calculated by multiplying the yield moment capacity by R_{bPr} from the proposed model discussed in Section 2.

In addition to the above, the bend-buckling stress of the longitudinally stiffened web, F_{crw}, is calculated using the AASHTO LRFD Article 6.10.1.9.2 provisions. If this stress is less than F_{yr} = $0.5F_{yc}$, the unbraced length at which the nominal elastic buckling stress F_{nc} is equal to F_{crw} is determined. The value F_{crw} is the stress level at which R_b effectively becomes equal to 1.0, and the corresponding unbraced length is referred to here as L_1. The inelastic LTB resistance of the longitudinally stiffened plate girder is then determined by linearly interpolating between the plateau strength (using the factor R_{bPr}) at L_p and the point (L_1, F_{crw}).

Conversely, if F_{crw} is greater than F_{yr} = $0.5F_{yc}$, the inelastic LTB resistance is obtained by linearly interpolating between (L_p, $R_{bPr}F_{yc}$) and (L_r, $0.5F_{yc}$), where L_r is defined here as the length at which the theoretical elastic LTB strength is equal to F_{yr} = $0.5F_{yc}$ (note that the current AASHTO provisions define L_r as the length corresponding to F_{yr} = $0.7F_{yc}$ for homogeneous slender web plate girders).

For compression flange stress levels below the smaller of the values F_{crw} or $0.5F_{yc}$, the elastic buckling equation in the current AASHTO Specifications, with R_b = 1 is used to compute the LTB resistance.

4.2 Case Studies

The cases defined in Table 1 are assessed as part of the parametric studies discussed in this paper. The unbraced length is different for each of these cases. The different KL_b values shown in the table belong to different ranges of the AASHTO LTB curve depending on the girder dimensions (particularly the b_{fc}/D ratio) for a given test. In general, Case 1 has an effective

unbraced length near the transition between the yield plateau and the inelastic lateral torsional buckling regions as defined by AASHTO (i.e., at the length $KL_b = L_p$). Cases 2 and 3 have effective unbraced lengths within the inelastic LTB range. Case 4 has an effective unbraced length near the length L_r on the current AASHTO LTB curve, but located in either the inelastic or elastic LTB region depending on the girder dimensions. Cases 5, 6 and 7 are comprised of studies with effective unbraced lengths well within the elastic range of the AASHTO LTB resistance curve.

Table 1: Case studies for straight longitudinally stiffened girders at the LTB limit state

Case	KL_b (in) d_o/D =1
1	225
2	375
3	525
4	675
5	825
6	975
7	1125[1]

1. Unbraced length studied only for girders with D/t_w = 300, and D/b_{fc} = 5, 4

For each of the above cases, the following parameters are held constant:

- D = 150 inches,
- d_s/D_c = 0.4, which is the theoretical optimum position for flexure (Dubas 1948; Massonnet 1960).
- Longitudinal stiffeners sized based on the minimum requirements from the AASHTO LRFD Specifications, and
- 9.5 x 0.75 inch transverse stiffeners, which satisfy the minimum requirements from the AASHTO LRFD Specifications for all of the girders tested.

The following parameters are varied:

- D_c/D = 0.5, 0.625 and 0.75,
- D/t_w = 200, 240 and 300, and
- b_{fc} = D/6, D/5, and D/4.
- t_{fc} = 1.5, 1.75, 2.25 in corresponding to the different values of compression flange widths.

A total of 168 test girders are studied for LTB in this paper.

4.3 Summary of Results

Figures 6 through 8 compare the FE test simulation data for three cross-sections to the current AASHTO LRFD and Eurocode predictions as well as to the above proposed model for several tests with d_o/D =1. These figures show comparisons between the data obtained using the imperfections as per the full AWS tolerances and the full Best-Fit Prawel residual stresses, and with half of the AWS tolerances as imperfections and half Best-Fit Prawel residual stresses. Subramanian and White (2015a) recommend using one-half of the Best-Fit Prawel pattern

residual stresses along with half the AWS tolerances as initial geometric imperfections to capture the mean of experimental data for LTB of unstiffened girders. There is no statistical data available on the residual stress distributions present in longitudinally stiffened girders. The proposed LTB model in Section 4.1 is shown to be conservative with respect to the test simulation data that use one-half of the residual stresses along with one-half the imperfections. The results presented in this paper, using the full magnitude of residual stresses shown in Fig. 5 and the imperfection magnitudes shown in Fig. 4, provide results that are closer to the lower bound of test simulation data using other combinations of residual stresses and imperfections within the AWS tolerances.

In the following figures and discussions, M_{max} refers to the flexural capacity obtained from FE test simulations, M_n *EC* refers to the capacity calculated using the Eurocode EN 1993-1-1 (CEN 2005) and EN 1993-1-5 (CEN 2006) provisions, M_n *AASHTO* (R_b based on F_{yc}) is the capacity computed using the current AASHTO provisions including R_b as calculated by AASHTO, as well as using the elastic section modulus that includes the longitudinal stiffener, M_n *AASHTO* (R_b = 1.0) is the same calculation but taking R_b = 1.0, and M_n *Proposed* is the result from the proposed model described in Section 4.1. In these figures, the data points that correspond to the "plateau resistance" are obtained from the results in Subramanian and White (2014).

The Commentary to Article 6.10.1.10.2 of the AASHTO LRFD Specifications permits the use of the compression flange stress at the governing strength condition in place of F_{yc} in the calculation of R_b in case of LTB or FLB, when the compression flange stress is smaller than F_{yc}. This approach recognizes the fact that the postbuckled web is generally more effective when the compression flange stress is smaller than F_{yc} at the governing strength condition. However, since the expression for R_b in AASHTO (2015) is derived for non-longitudinally stiffened girders, and is extremely conservative (20 to 60%) for longitudinally stiffened girders (Subramanian and White 2016), the approach of using a slightly larger R_b based on a compression flange stress smaller than F_{yc} does not yield a significant increase in strength. Hence, in this paper, the simplified calculation of R_b based on F_{yc} is presented when plotting M_n AASHTO based on $R_b \leq 1$.

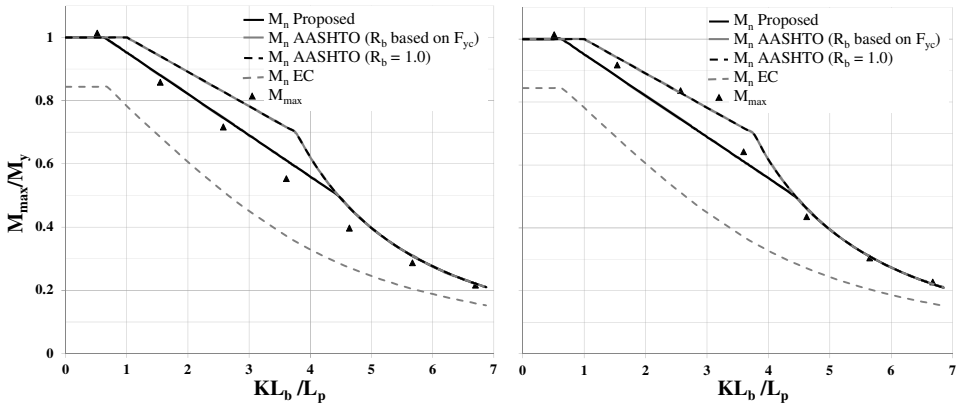

Figure 6: Flexural capacity comparing AASHTO, Eurocode and FE simulations, D/t_w = 240, D_c/D = 0.5, D/b_{fc} = 6, d_o/D = 1 with full AWS imperfections and Best-fit Prawel residual stress (Left) and half AWS imperfections and half Best-fit Prawel residual stress (right)

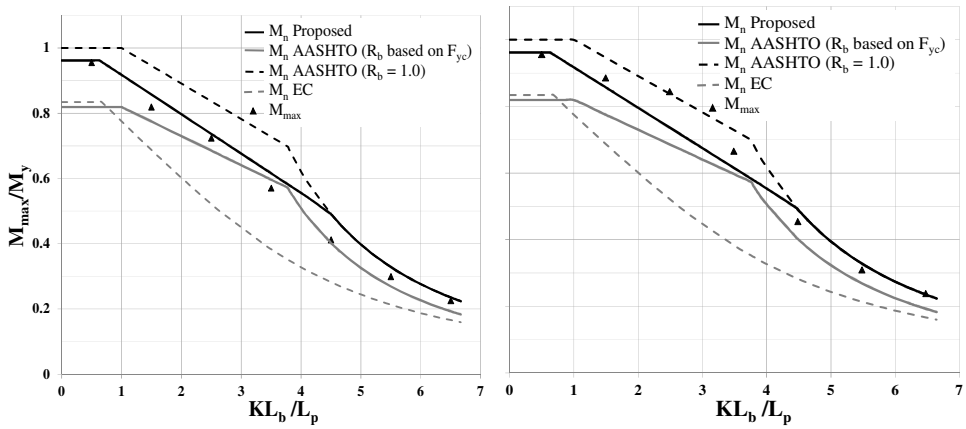

Figure 7: Flexural capacity comparing AASHTO, Eurocode and FE simulations, D/t_w = 300, D_c/D = 0.5, D/b_{fc} = 6, d_o/D = 1 with full AWS imperfections and Best-fit Prawel residual stress (Left) and half AWS imperfections and half Best-fit Prawel residual stress (right)

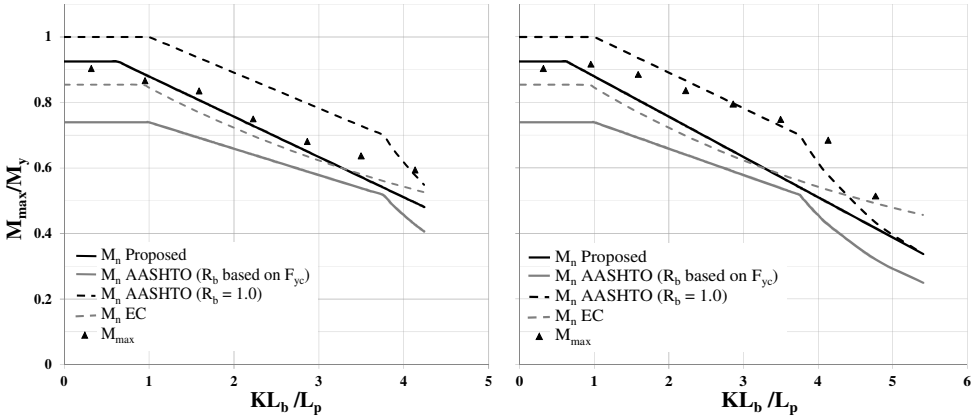

Figure 8: Flexural capacity comparing AASHTO, Eurocode and FE simulations, D/t_w = 300, D_c/D = 0.75, D/b_{fc} = 4, d_o/D = 1 with full AWS imperfections and Best-fit Prawel residual stress (Left) and half AWS imperfections and half Best-fit Prawel residual stress (right)

Figure 6 shows results for a girder that has a value of $R_{bAASHTO}$ = 1.0 ($R_{bAASHTO}$ is equal to 1.0 here because the longitudinal stiffener increases the bend-buckling stress F_{crw} to a value greater than the compression flange stress at the strength limit for all unbraced lengths).

Figures 7 and 8 show results for slender web longitudinally stiffened girders where $R_{bAASHTO}$ < 1.0. It can be observed from Fig. 7 that at the point (L_1, $F_{crw}S_{xc}$), the M_n *AASHTO* (R_b = *1.0*) curve tends to over-predict the LTB resistance of the girders obtained from the test simulations. One can observe that the proposed model is also somewhat unconservative near this point, since the proposed model and the above AASHTO model both correspond to the theoretical elastic LTB resistance (with J taken equal to zero) at (L_1, F_{crw}). This over-prediction by the proposed model is greatly reduced in the plots on the right that correspond to one-half the AWS tolerances used as imperfections, and one-half Best-fit Prawel residual stresses. Furthermore, the proposed model still slightly over predicts the test simulation results for shorter unbraced lengths within the inelastic LTB for these higher values of initial geometric imperfections. The M_n *AASHTO* (R_b based on F_{yc}) curve gives a closer prediction to the test simulation results in the vicinity of KL_b =

L_1. However, this is largely because a single R_b is calculated conservatively by taking the compression flange stress as F_{yc} and then used throughout this curve. The M_n *AASHTO* (R_b based on F_{yc}) curve is significantly conservative for short effective unbraced lengths.

In the case of singly-symmetric girders having a large tension flange (and hence a large D_c/D), the AASHTO LRFD and proposed equations are highly conservative for large KL_b values when $R_{bAASHTO} < 1.0$ as shown in Fig. 8. This is owed to the AASHTO and AISC based assumption that, due to the slender web and potential distortional lateral buckling, the St. Venant torsional stiffness GJ provides negligible help to the LTB resistance. The AASHTO equations neglect the contribution from St. Venant torsion in calculating the elastic buckling stress for all slender web I-sections. This is a conservative approximation for the girders with large tension flanges studied in this research. For these girders, it is notable that the FE predictions compare closely with the calculations based on Eurocode, in which the authors include the St. Venant torsional stiffness contribution to the LTB resistance.

It is important to note that the above behavior for large tension flanges may not always be the case. Due to the cross-section distortional deflection of the web, the influence of GJ on I-girder LTB resistances can be substantially reduced (White and Jung 2007). However, for longitudinally stiffened girders having relatively close spacing of the intermediate transverse stiffeners, the frame action of the transverse stiffeners may be expected to limit the amount and impact of the distortional deflections of the web. The authors have subsequently conducted studies on a larger panel aspect ratio of $d_o/D = 2.0$, and found that distortional deflections do not greatly influence the capacities of these types of members (Subramanian 2015).

In addition, the above plots indicate that, in many cases, the Eurocode is conservative in its prediction of the LTB resistances of longitudinally stiffened girders obtained from the test simulations conducted in this research. This is chiefly due to the assumption of larger flange residual stresses in similar underlying test simulations conducted in the research leading to the Eurocode provisions (Greiner et al. 2001). The best estimate of the FE test simulation results conducted in this research is obtained using the proposed model.

Table 2 summarizes the moment capacities obtained for all the doubly-symmetric girders ($D_c/D = 0.5$) for the panel aspect ratios of 1.0, evaluated in the LTB test simulations, while also addressing how well the AASHTO, Eurocode, and proposed model compare to the simulation data (M_{max}). It is observed that the proposed LTB model described in Section 4.1 performs better than the current AASHTO and Eurocode equations in predicting the simulation-based flexural capacities of these girders. The results discussed in Table 2 are based on one-half AWS tolerances as imperfections along with one-half Best-Fit Prawel residual stresses.

Table 2: Statistics for 27 longitudinally stiffened girders

(a) $KL_b = 225$ in

Statistical Parameter	$D_c/D = 0.5$			$D_c/D = 0.625$			$D_c/D = 0.75$		
	M_{max} / $M_{nProposed}$	M_{max} / $M_{nAASHTO}$	M_{max} / M_{nEC}	M_{max} / $M_{nProposed}$	M_{max} / $M_{nAASHTO}$	M_{max} / M_{nEC}	M_{max} / $M_{nProposed}$	M_{max} / $M_{nAASHTO}$	M_{max} / M_{nEC}
Mean	1.05	1.04	1.26	1.05	1.13	1.21	1.05	1.30	1.16
COV	0.02	0.06	0.06	0.01	0.10	0.04	0.01	0.08	0.05
Maximum	1.08	1.14	1.36	1.07	1.26	1.28	1.07	1.51	1.25
Minimum	1.03	0.98	1.15	1.03	0.96	1.11	1.03	1.18	1.08

Table 2 (Continued): Statistics for 27 longitudinally stiffened girders

(b) KL_b = 375 in

Statistical Parameter	D_c/D = 0.5			D_c/D = 0.625			D_c/D = 0.75		
	M_{max} / $M_{nProposed}$	M_{max} / $M_{nAASHTO}$	M_{max} / M_{nEC}	M_{max} / $M_{nProposed}$	M_{max} / $M_{nAASHTO}$	M_{max} / M_{nEC}	M_{max} / $M_{nProposed}$	M_{max} / $M_{nAASHTO}$	M_{max} / M_{nEC}
Mean	1.11	1.07	1.46	1.12	1.18	1.36	1.17	1.41	1.31
COV	0.02	0.08	0.09	0.02	0.12	0.07	0.04	0.11	0.07
Maximum	1.15	1.23	1.63	1.17	1.40	1.48	1.23	1.71	1.44
Minimum	1.08	1.01	1.28	1.08	1.00	1.21	1.10	1.25	1.15

(c) KL_b = 525 in

Statistical Parameter	D_c/D = 0.5			D_c/D = 0.625			D_c/D = 0.75		
	M_{max} / $M_{nProposed}$	M_{max} / $M_{nAASHTO}$	M_{max} / M_{nEC}	M_{max} / $M_{nProposed}$	M_{max} / $M_{nAASHTO}$	M_{max} / M_{nEC}	M_{max} / $M_{nProposed}$	M_{max} / $M_{nAASHTO}$	M_{max} / M_{nEC}
Mean	1.10	1.02	1.60	1.13	1.15	1.42	1.23	1.47	1.35
COV	0.03	0.09	0.08	0.03	0.12	0.05	0.05	0.12	0.08
Maximum	1.14	1.16	1.74	1.18	1.32	1.48	1.32	1.77	1.50
Minimum	1.04	0.88	1.43	1.07	0.93	1.32	1.15	1.26	1.20

(d) KL_b = 675 in

Statistical Parameter	D_c/D = 0.5			D_c/D = 0.625			D_c/D = 0.75		
	M_{max} / $M_{nProposed}$	M_{max} / $M_{nAASHTO}$	M_{max} / M_{nEC}	M_{max} / $M_{nProposed}$	M_{max} / $M_{nAASHTO}$	M_{max} / M_{nEC}	M_{max} / $M_{nProposed}$	M_{max} / $M_{nAASHTO}$	M_{max} / M_{nEC}
Mean	1.04	1.00	1.63	1.10	1.18	1.39	1.33	1.71	1.35
COV	0.08	0.09	0.02	0.05	0.14	0.05	0.08	0.25	0.10
Maximum	1.14	1.13	1.69	1.17	1.45	1.46	1.53	2.37	1.55
Minimum	0.93	0.87	1.59	1.01	0.94	1.27	1.21	1.30	1.22

(e) KL_b = 825 in

Statistical Parameter	D_c/D = 0.5			D_c/D = 0.625			D_c/D = 0.75		
	M_{max} / $M_{nProposed}$	M_{max} / $M_{nAASHTO}$	M_{max} / M_{nEC}	M_{max} / $M_{nProposed}$	M_{max} / $M_{nAASHTO}$	M_{max} / M_{nEC}	M_{max} / $M_{nProposed}$	M_{max} / $M_{nAASHTO}$	M_{max} / M_{nEC}
Mean	0.99	0.99	1.55	1.10	1.23	1.30	1.52	2.07	1.34
COV	0.07	0.08	0.05	0.06	0.16	0.09	0.15	0.30	0.11
Maximum	1.08	1.15	1.65	1.19	1.53	1.46	1.96	2.91	1.54
Minimum	0.90	0.92	1.44	0.98	0.96	1.17	1.31	1.36	1.16

(f) KL_b = 975 in

Statistical Parameter	D_c/D = 0.5			D_c/D = 0.625			D_c/D = 0.75		
	M_{max} / $M_{nProposed}$	M_{max} / $M_{nAASHTO}$	M_{max} / M_{nEC}	M_{max} / $M_{nProposed}$	M_{max} / $M_{nAASHTO}$	M_{max} / M_{nEC}	M_{max} / $M_{nProposed}$	M_{max} / $M_{nAASHTO}$	M_{max} / M_{nEC}
Mean	1.00	1.03	1.51	1.15	1.33	1.24	1.72	2.46	1.28
COV	0.03	0.10	0.05	0.07	0.17	0.09	0.21	0.32	0.11
Maximum	1.06	1.24	1.60	1.31	1.71	1.40	2.35	3.54	1.47
Minimum	0.97	0.91	1.43	1.06	1.02	1.11	1.32	1.59	1.10

(g) KL_b = 1125 in (6 girders)

Statistical Parameter	D_c/D = 0.5			D_c/D = 0.625			D_c/D = 0.75		
	M_{max} / $M_{nProposed}$	M_{max} / $M_{nAASHTO}$	M_{max} / M_{nEC}	M_{max} / $M_{nProposed}$	M_{max} / $M_{nAASHTO}$	M_{max} / M_{nEC}	M_{max} / $M_{nProposed}$	M_{max} / $M_{nAASHTO}$	M_{max} / M_{nEC}
Mean	0.97	1.11	1.47	1.07	1.36	1.19	1.52	2.22	1.24
COV	0.04	0.07	0.04	0.12	0.18	0.02	0.27	0.39	0.22
Maximum	1.00	1.17	1.51	1.16	1.54	1.21	1.81	2.84	1.43
Minimum	0.95	1.05	1.42	0.98	1.19	1.17	1.24	1.60	1.05

Summary of results for doubly-symmetric girders

From Table 2, it is observed that the proposed model described in Section 4.1 performs better than the current AASHTO and Eurocode equations in predicting the simulation-based flexural capacities of these girders. The following key points are gleaned from the above table:

1. The proposed model performs reasonably well for doubly-symmetric slender web girders. In general, this model gives slightly conservative predictions at smaller unbraced lengths in the inelastic LTB region, as compared to the AASHTO equations. This is due to the low values of initial geometric imperfections and residual stresses used in FE test simulations. As noted previously, due to end fixities on the test specimen, an initial flange sweep of $L_b/2000$ is close to $L_b/4000$ between the inflection points. The influence of this low magnitude of imperfection is reflected in Figs. 6 through 8, where the simulation data indicate a relatively flat slope within the inelastic LTB region for the plots shown on the right. However, plots for twice the values of initial imperfections are also shown in Figures 6 through 8 (left), which indicate excellent correlation with the proposed model in the inelastic range, although slightly unconservative at the region around L_r. In view of these observations, it is reasonable to state that the proposed LTB model is safe to use for design in the presence of geometric imperfections within AWS tolerances.
2. While the current AASHTO model is conservative for the yield limit state, it tends to over-predict the capacities for the doubly-symmetric girders in the inelastic and the shorter lengths of the elastic regions of the LTB curve (minimum of $M_{max}/M_{nAASHTO}$ ranges from 0.87 to 0.91). The current AASHTO predictions are actually quite good for doubly-symmetric girders at the smallest unbraced length considered within the inelastic LTB range in these studies (KL_b = 225 inches and 300 inches, Table 2) and the longest unbraced lengths within the elastic LTB region (KL_b = 1125 inches).

   It is important to note that the $M_{nAASHTO}$ calculations here are based on the calculation of a single R_b using the compression flange yield strength, and the use of this R_b for all the unbraced lengths corresponding to a given girder cross-section is conservative. If separate larger R_b values are calculated for each of the unbraced lengths, as permitted by AASHTO LRFD Article C6.10.1.10.2, the current AASHTO LRFD predictions tend to increase for larger KL_b values within the inelastic buckling range, but not sufficiently large to capture the strengths indicated by FE test simulations.
3. The proposed model recognizes the fact that R_b =1 at effective unbraced lengths long enough where the elastic LTB strength precedes web bend-buckling. This ensures that the proposed model is either an excellent prediction of elastic LTB strengths (for doubly-symmetric girders) or conservative (for singly-symmetric girders with large tension flanges) at large effective unbraced lengths.

Summary of results for singly-symmetric girders

The following key points are gleaned from the Table 2 for singly-symmetric cross-sections.

1. The current AASHTO LRFD equations can severely under-predict the true strength in the case of singly-symmetric girders, especially at longer unbraced lengths in the elastic buckling range. The mean professional factor ($M_{max}/M_{nAASHTO}$) for D_c/D = 0.625 varies between 1.13 and 1.36, and the COV varies between 0.10 and 0.18. The mean professional factor ($M_{max}/M_{nAASHTO}$) for D_c/D = 0.75 varies between 1.3 and 2.46, and the COV varies between 0.08 and 0.39. The larger means and COVs are for the longer unbraced lengths. It is evident

that neglecting J in computing the elastic unbraced lengths is overly pessimistic for cross-sections with larger tension flanges. However, including J and using the form of the proposed or current LTB strength equations, will result in a gross over-prediction of the inelastic LTB strength of such girders.

2. The proposed model provides a better prediction with a mean professional factor ($M_{max}/M_{nProposed}$) that varies between 1.05 and 1.15, and a COV that varies between 0.01 and 0.12 for $D_c/D = 0.625$. The mean professional factor ($M_{max}/M_{nProposed}$) for $D_c/D = 0.75$ varies between 1.05 and 1.72, and the COV varies between 0.01 and 0.27.
3. The current AASHTO model under-predicts the capacity for several reasons. The first is that AASHTO's current calculation of R_b is highly conservative for singly-symmetric girders as discussed in Subramanian and White (2014). The second is the fact that the AASHTO elastic LTB equations neglect the St Venant torsional stiffness (GJ) contribution to the buckling strength. These factors combine to make the current AASHTO predictions significantly conservative for these cases.
4. The proposed model eliminates the conservatism associated with the first of the above reasons. However, it does not address the second reason. As discussed previously, one must be cautious in counting upon the contribution from GJ for slender web members. However, it is expected that for the close transverse stiffener spacing typically used in longitudinally stiffened girders (even if the AASHTO d_o/D limit is extended to 2.0), the assumption of $J = 0$ in writing the LTB resistances tends to be generally conservative.

   For the singly-symmetric girders studied in this research, the above conservative approach of taking $J = 0$ in the elastic LTB prediction is justified due to lack of better characterization of web distortion effects.

Based on the data in Table 2, one can observe that the Eurocode model is more conservative than the test simulation data, and the proposed model for $D_c/D = 0.5$, and $D_c/D = 0.625$. However, the under-prediction by the Eurocode model is consistent across various unbraced lengths for singly-symmetric girders and is larger for doubly-symmetric cross-sections in the inelastic and elastic LTB region. This conservatism is largely due to two reasons:

1. For slender web girders with unbraced lengths sufficiently short such that the yield limit state governs, the Eurocode effective width cross-section model (CEN 2006) is conservative compared to the proposed cross-section R_b model in Section 2 (Subramanian and White 2016).
2. The residual stress pattern considered for slender web I-girders in the Eurocode developments is more severe than that considered in this research (Greiner et al. 2001).

The Eurocode predictions are less conservative than the proposed model for cross-sections with $D_c/D = 0.75$ at long unbraced lengths in the elastic LTB region because, the calculations presented in this paper for M_{nEC} include the effect of the St.Venant torsional rigidity, GJ. The proposed model and AASHTO equations take GJ to be zero for these types of members.

5. Flange Local Buckling Limit State

Selected tests are conducted to assess the performance of the proposed R_b cross-section model in Section 2 while evaluating the strengths of longitudinally stiffened plate girders that are controlled by the Flange Local Buckling (FLB) limit state. AASHTO (2015) restricts the flange slenderness ($b_{fc}/2t_{fc}$) to 12 in Section 6.11.2.2. This limit ensures that the members studied in this

paper are noncompact flange cross-sections. The paper examines the applicability of the flange local buckling resistance in the current AASHTO provisions for longitudinally stiffened homogenous girders.

The FLB resistance equations are given in Section 6.10.8.2.2 of the AASHTO Specifications. When the compression flange is compact, the local buckling resistance of the flange is taken as $R_b F_{yc}$. In case of a noncompact flange, AASHTO Equation 6.10.8.2.2-2,

$$F_{nc} = \left[1 - \left(1 - \frac{F_{yr}}{R_h F_{yc}}\right)\left(\frac{\lambda_f - \lambda_{pf}}{\lambda_{rf} - \lambda_{pf}}\right)\right] R_b R_h F_{yc} \tag{2}$$

is used to compute the local buckling resistance of the flange. The applicability of this equation in conjunction with the proposed R_b model is discussed below.

5.1 FE Modeling

The same test setup used in Fig. 3 is used in the FLB studies. The lateral braces at the compression flange are spaced such that the unbraced length is smaller than the plateau length, L_p.

The Best-Fit Prawel residual stresses and the longitudinal stiffener residual stress as shown in Fig. 5 are used in the FLB test studies. The initial web-out-flatness imperfections used in these tests are also modeled via the same procedure described previously. In addition to the web imperfection, a flange tilt as shown in Fig. 4 (b) is modeled for the FLB sensitive studies in this chapter, also satisfying the AWS (2010) criteria.

5.2 Case Studies

Two cases with d_o/D = 1, and 2 are selectively studied for validating the FLB equations. They are designated as Cases 1, and 2 in Table 3. The compression flange slenderness, $b_{fc}/2t_{fc}$ is set to 12.0 for all the girders studied here. The following parameters are varied here.

- D_c/D = 0.5, 0.625 and 0.75,
- D/t_w = 200, 240 and 300, and
- b_{fc} = D/6, D/5 and D/4.
- t_{fc} = 1.04, 1.25 and 1.57 corresponding to the three different values of b_{fc}.

The clear web depth between the flanges is 150 in, and the yield stress of all the plate elements is 50 ksi. The longitudinal stiffener is located at $0.4D_c$. A total of 54 girders are studied for FLB in this paper.

Table 3: Case studies for straight girders at FLB limit state

Case	d_o/D	Longitudinal Stiffener	d_s/D_c
1	1	AASHTO min	0.4
2	2	AASHTO min	0.4

5.3 Results

The results of this study are tabulated in Tables 4 and 5 for Cases 1 and 2. The results are presented as a comparison between M_{max}/M_{nPr} and $M_{max}/M_{nAASHTO}$, where M_{max} is the maximum

moment obtained in the FE test simulation, M_{nPr} is the flange local buckling capacity calculated using R_{bPr} in conjunction with AASHTO (2015) FLB equations and $M_{nAASHTO}$ is calculated using $R_{bAASHTO}$.

It is evident from Tables 4 and 5, and from Fig. 9 that the proposed R_b model provides satisfactory, albeit conservative predictions (11 to 17%) of the girder resistances for noncompact flange longitudinally stiffened girders compared to test simulations. It is also clear that the AASHTO equations tend to under-predict the true capacities by a larger margin (11 to 71%) than the proposed model by virtue of the fact that R_b is conservative for doubly-symmetric longitudinally stiffened girders, and more so for singly-symmetric members, as demonstrated in Subramanian and White (2014).

Table 4: Comparison of FLB capacities using R_{bPr} and $R_{bAASHTO}$ for Case 1

(a): $D/t_w = 300$

D_c/D	D/b_{fc}	M_{max}/M_{nPr}	$M_{max}/M_{nAASHTO}$
0.5	6	1.11	1.28
	5	1.12	1.26
	4	1.13	1.22
0.625	6	1.12	1.42
	5	1.11	1.33
	4	1.11	1.25
0.75	6	1.11	1.64
	5	1.11	1.49
	4	1.11	1.34

(b): $D/t_w = 240$

D_c/D	D/b_{fc}	M_{max}/M_{nPr}	$M_{max}/M_{nAASHTO}$
0.5	6	1.11	1.11
	5	1.14	1.14
	4	1.14	1.14
0.625	6	1.14	1.38
	5	1.16	1.34
	4	1.14	1.26
0.75	6	1.13	1.50
	5	1.14	1.42
	4	1.06	1.23

(c): $D/t_w = 200$

D_c/D	D/b_{fc}	M_{max}/M_{nPr}	$M_{max}/M_{nAASHTO}$
0.5	6	1.17	1.17
	5	1.16	1.16
	4	1.17	1.17
0.625	6	1.11	1.11
	5	1.13	1.13
	4	1.14	1.14
0.75	6	1.14	1.42
	5	1.15	1.38
	4	1.16	1.32

Table 5: Comparison of FLB capacities using R_{bPr} and $R_{bAASHTO}$ for Case 2

(a): $D/t_w = 300$

D_c/D	D/b_{fc}	M_{max}/M_{nPr}	$M_{max}/M_{nAASHTO}$
0.5	6	1.15	1.33
	5	1.14	1.28
	4	1.11	1.20
0.625	6	1.14	1.46
	5	1.15	1.39
	4	1.13	1.28
0.75	6	1.13	1.71
	5	1.14	1.56
	4	1.12	1.37

(b): $D/t_w = 240$

D_c/D	D/b_{fc}	M_{max}/M_{nPr}	$M_{max}/M_{nAASHTO}$
0.5	6	1.12	1.12
	5	1.11	1.11
	4	1.14	1.14
0.625	6	1.15	1.41
	5	1.16	1.36
	4	1.15	1.29
0.75	6	1.13	1.54
	5	1.15	1.47
	4	1.16	1.37

(c): $D/t_w = 200$

D_c/D	D/b_{fc}	M_{max}/M_{nPr}	$M_{max}/M_{nAASHTO}$
0.5	6	1.13	1.13
	5	1.11	1.11
	4	1.10	1.10
0.625	6	1.14	1.14
	5	1.16	1.16
	4	1.17	1.17
0.75	6	1.14	1.46
	5	1.16	1.42
	4	1.17	1.35

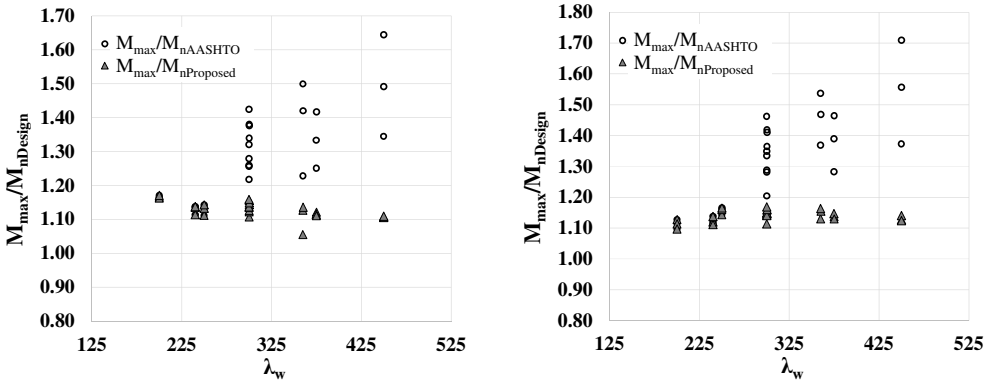

(a) Case 1, d_o/D =1, d_s/D_c = 0.4 (b) Case 2, d_o/D =2, d_s/D_c = 0.4

Figure 9: Comparison of $M_{nProposed}$ with $M_{nAASHTO}$ for FLB of longitudinally stiffened girders

It is recommended, based on the tests discussed in this paper, that the same form of the equations as in the current Specifications be used for FLB resistance calculations. However, R_b may be computed using the proposed R_b cross-section model.

Table 6 shows the overall statistics of the proposed R_b model and the current AASHTO equations for longitudinally stiffened girders governed by the FLB limit state. Clearly, the proposed model is more optimistic than the AASHTO equations, with a lower mean and a lower coefficient of variation.

Table 6: Statistics for M_{max}/M_{nPr} and $M_{max}/M_{nAASHTO}$ for straight girders at FLB limit state

Statistical Parameter	M_{max}/M_{nPr}	$M_{max}/M_{nAASHTO}$
Mean	1.13	1.30
COV	0.02	0.12
Maximum	1.17	1.71
Minimum	1.06	1.10
Median	1.14	1.29

6. Conclusions

A proposed cross-section model to calculate R_b of longitudinally stiffened girders is evaluated for LTB and FLB limit states in this paper. The following conclusions can be drawn from the research presented herein.

1. This paper demonstrates that using the superior R_b cross-section model along with modified LTB equations predicts the LTB strengths of straight longitudinally stiffened girders obtained from FE simulations better than the current AASHTO and Eurocode equations. The proposed modified form of the LTB equations gives due consideration to the occurrence of web bend-buckling, and provides a much improved correlation with test simulation data when compared to the AASHTO 2015 Specifications. This model also explicitly recognizes that the load shedding factor, R_b, need not be used as a factor on the LTB resistance equations, if LTB precedes web bend-buckling.
2. It is established that the proposed R_b model used in conjunction with the FLB equations for noncompact flanges is satisfactory in predicting the capacities of these types of girders. Slender flanges are not studied in this research because AASHTO effectively prohibits their use in bridge girders by limiting the maximum flange slenderness to 12.0.

The authors have also conducted research with moment gradient loading in subsequent research, and have shown that the proposed cross-section model for R_b can satisfactorily be used for all loading and limit state conditions for straight longitudinally stiffened girders.

References

AASHTO (2015). *AASHTO LRFD Bridge Design Specifications. 7th Edition*, American Association of State Highway and Transportation Officials, Washington, DC.

AISC (2010). *Code of Standard Practice for Steel Buildings and Bridges, AISC 303-05*, American Institute of Steel Construction, Chicago, IL.

AWS (2010). *Structural Welding Code–Steel, AWS D1.1: D1.1M, 22nd ed*, AWS Committee on Structural Welding.

Basler, K., and Thurliman, B. (1961). "Strength of Plate Girders in Bending." *Journal of Structural Division - American Society of Civil Engineers*, 87(ST6), 153-181.

CEN (2005). *Design of Steel Structures, Part 1-1: General Rules and rules for buildings, EN 1993-1-1:2005:E, Incorporating Corrigendum February 2006*, European Committee for Standardization, Brussels, Belgium.

CEN (2006). *Eurocode 3: Design of Steel Structures, Part 1-5: General Rules - Plated Structural Elements, EN 1993-1-5:2006: E, Incorporating Corrigendum April 2009*, European Committee for Standardization, Brussels, Belgium.

Cooper, P. B. (1965). "Bending and Shear Strength of Longitudinally Stiffened Plate Girders." Fritz Engineering Laboratory Rep. No. 304.6, Lehigh University ., Bethlehem, Pa.

Dubas, C. (1948). "Contribution A` L' E'tude Du Voilement Des To`les Raidies (A Contribution to the Buckling of Stiffened Plates)." *IABSE Preliminary Publication. Third Congress, International Association for Bridge and Structural Engineers*.

Greiner, R., Salzgeber, G., and Ofner, R. (2001). "New lateral torsional buckling curves κ_{LT}-numerical simulations and design formulae." ECCS TC8, Report 30, June 2000 (rev), 43.

Hendy, C. R., and Murphy, C. J. (2007). *Designers' Guide to EN 1993-2 Eurocode 3: Design of steel structures. Part 2: Steel bridges*, Thomas Telford Publishing, Thomas Telford Ltd, London.

Kim, Y. D. (2010). "Behavior and Design of Metal Building Frames Using General Prismatic and Web-Tapered Steel I-Section Members."Doctoral Dissertation, Georgia Institute of Technology, Atlanta, GA.

Massonnet, C. E. L. (1960). "Stability considerations in the Design of Steel Plate Girders." *Journal of Structural Division - American Society of Civil Engineers*, 86(ST1), 71-97.

Simulia (2013). *ABAQUS/Standard Version 6.12-1*, Simulia, Inc, Providence, RI.

Subramanian, L. P. (2015). "Flexural Resistance of Longitudinally Stiffened Plate Girders."Doctoral Dissertation, Georgia Institute of Technology, Atlanta, GA.

Subramanian, L. P., Jeong, W. Y., Yellepeddi, R., and White, D. W. (2016). "Assessment of I-Section Member LTB Experimental Tests Using Inelastic Buckling Analysis." *Structural Engineering, Mechanics and Materials Report No. 110*, School of Civil and Environmental Engineering, Georgia Institute of Technology, Atlanta, GA.

Subramanian, L. P., and White, D. W. (2014). "Web Post Buckling resistance of Longitudinally Stiffened Plate Girders." *Annual Stability Conference*, Structural Stability Research Council, Toronto, Canada.

Subramanian, L. P., and White, D. W. (2015). "Sensitivity of I-Section Member Lateral Torsional Buckling Resistances to Geometric Imperfections and Residual Stresses." *Structural Engineering, Mechanics and Materials Report No. 106*, School of Civil and Environmental Engineering, Georgia Institute of Technology, Atlanta, GA.

Subramanian, L. P., and White, D. W. (2015a). "Evaluation of Lateral Torsional Buckling Resistance Equations in AISC and AASHTO " *Annual Stability Conference*, Structural Stability Research Council, Nashville, Tennessee.

Subramanian, L. P., and White, D. W. (2015b). "A Reassessment of the LTB Resistance of Rolled I-Section Members - Uniform Moment Tests." *Structural Engineering, Mechanics and Materials Report No. 107*, School of Civil and Environmental Engineering, Georgia Institute of Technology, Atlanta, GA.

Subramanian, L. P., and White, D. W. (2015c). "A Reassessment of the LTB Resistance of Rolled I-Section Members - Moment Gradient Tests." *Structural Engineering, Mechanics and Materials Report No. 109*, School of Civil and Environmental Engineering, Georgia Institute of Technology, Atlanta, GA.

Subramanian, L. P., and White, D. W. (2016). "A Reassessment of the Maximum Potential Flexural Resistance of Longitudinally Stiffened I-Girders." *Structural Engineering, Mechanics and Materials Report No. 111*, School of Civil and Environmental Engineering, Georgia Institute of Technology, Atlanta, GA.

White, D. W., and Jung, S.-K. (2007). "Effect of web distortion on the buckling strength of noncomposite discretely-braced steel I-section members." *Engineering Structures*, 29(8), 1872-1888.